H. Shangguan, L. W. Casperson, A. Shearin, S. A. Prahl, "Investigation of cavitation bubble dynamics using particle image velocimetry: implications for photoacoustic drug delivery," in *SPIE Proceedings of Lasers in Surgery: Advanced Characterization, Therapeutics, and Systems VI*, R. R. Anderson, A. Katzir, **2671**, pp. 104–115, (1996).

Investigation of Cavitation Bubble Dynamics Using Particle Image Velocimetry: Implications for Photoacoustic Drug Delivery

HanQun Shangguan[1,2], Lee W. Casperson[1], Alan Shearin[2], and Scott A. Prahl[2,3,4]

[1]Portland State University, Department of Electrical Engineering, Portland, OR 97207
[2]Oregon Medical Laser Center, Portland, OR 97225
[3]Oregon Graduate Institute, Portland, OR 97291
[4]Oregon Health Sciences University, Portland, OR 97201

ABSTRACT

Photoacoustic drug delivery is a technique for delivering drugs to localized areas in the body. In cardiovascular applications, it uses a laser pulse to generate a cavitation bubble in a blood vessel due to the absorption of laser energy by targets (e.g., blood clots) or surrounding liquids (e.g., blood or injected saline). The hydrodynamic pressure arising from the expansion and collapse of the cavitation bubble can force the drug into the clots and tissue wall tissue. Time-resolved particle image velocimetry was used to investigate the flow of liquids during the expansion and collapse of cavitation bubbles near a soft boundary. A gelatin-based thrombus model was used to simulate the blood clot present during laser thrombolysis. An argon laser chopped by an acousto-optic modulator was used for illumination and photography was achieved using a CCD camera. The implications of this phenomenon on practical photoacoustic drug delivery implementation are discussed.

Keywords: localized drug delivery, high speed photography, hydrodynamic flow

1 INTRODUCTION

In our previous studies, we described a technique for delivering drugs to localized areas.[1–3] A series of laser pulses were used to generate cavitation bubbles in a blood vessel due to the absorption of laser energy by targets (e.g., blood clots) or surrounding liquids (e.g., blood or saline). The hydrodynamic pressure arising from the expansion and collapse of cavitation bubbles forced drug into clot or vessel wall. This technique is termed as photoacoustic drug delivery. The interest in the dynamics of cavitation bubbles in liquids arises from their importance in photoacoustic drug delivery.

Conventional flash photography and high speed photography have been widely used for the dynamics of laser-induced cavitation bubbles.[2,4–9] Unfortunately, a major limitation associated with these techniques is that it is impossible to track the temporal evolution of a fluid flow surrounding the cavitation bubble. To overcome this limitation, Vogel *et al.* demonstrated that the combination of particle image velocimetry (PIV) and high speed photography could be used to investigate the cavitation bubble dynamics near a solid boundary.[10] In this study, the images of the particles trajectories were recorded using a CCD camera. The use of a CCD camera makes

 0-8194-2045-X/96/$6.00

nearly real-time displays of stored information possible, which is helpful for monitoring the quality of images as experimental conditions change.

The aims of this study were to measure the velocities near laser-induced cavitation bubbles and investigate the hydrodynamic flow pattern arising from the cavitation bubble formation for the improvement of localized drug delivery.

2 Materials and Methods

2.1 Laser Systems

The experimental arrangement is outlined in Figure 1. A flashlamp-pumped dye laser (Palomar Medical Technologies) operating at 577 nm was used to create cavitation bubbles. The pulse duration was 1.3 μs (full width at half maximum). The laser pulses were delivered via a step-index fused silica optical fibers with 1000 μm core diameter. The laser energy was 60 mJ for the laser absorption on target and 30 mJ for the laser absorption at fiber tip (Figure 2). The light source for PIV was an argon-ion laser (Model 171, Spectra-Physics). Laser output was in the 2–8 W range before passing through an acousto-optic modulator (AOM-403c, Intra Action).

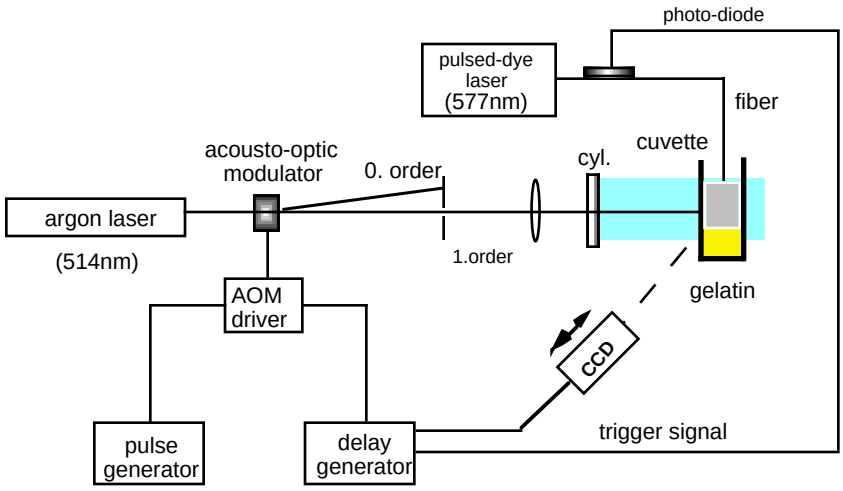

Figure 1: Experimental setup for time-resolved PIV of the flow around laser-induced cavitation bubbles

2.2 Cavitation Bubble Generation

The cavitation bubbles were formed either on gelatin (Figure 2(a)) or at fiber tip (Figure 2(b)). Laser absorption on gelatin was achieved by adding a light absorbing dye. Absorption of the fiber tip was achieved by painting a thin light absorbing layer (<200 μm) on the end face of the fiber tip. This made it possible to simulate the bubble formation typically found in light absorbing liquids and simultaneously allow visualization through the water. The fiber was located 1 mm above the gelatin target. The gelatin samples were covered with distilled water seeded with scatterers.

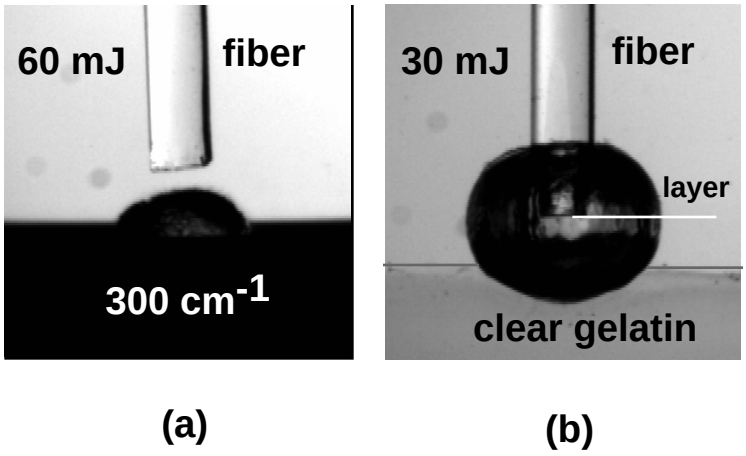

Figure 2: Schematic illustration of two configurations for cavitation bubble generation. (a) Laser absorption on gelatin. (b) Laser absorption at the fiber tip.

2.3 Thrombus Model

The thrombus was modeled using 10% gelatin (300 bloom). The percentage was determined by the weight ratio of gelatin to water. Samples were clear or blue color made by adding a dye (direct blue 15, Sigma). The gelatin-water mixture was heated to 60° C with stirring until it became clear, and then sufficient dye was added to achieve the desired absorption coefficient. For example, samples with $300\,\mathrm{cm}^{-1}$ could be made by adding 40 ml of distilled water, 4 g of the gelatin, and 0.231 g of the dye. Liquid gelatin samples were poured into 1 cm cuvettes and molded to form 2–3 cm thick thrombus models with planar geometry.

2.4 Scatterering Particles

The fluid was seeded with polymer microspheres (Duke Scientific) with an average diameter of $25\,\mu$m. These particles had nearly the same density as water ($1.05\,\mathrm{g/cm}^3$). Therefore, the particles would follow the flow arising from the expansion and collapse of cavitation bubbles. These particles were clear and did not absorb the laser energy, but could be visualized by the light that they scattered. The concentration of scatterers was about 3×10^4 scatterers/ml. It was difficult to ensure good spatial resolution in the analysis of the fluid velocity field if the concentration was greater than this value.

2.5 Particle Image Velocimetry

The laser beam from the argon laser was chopped by the acousto-optic modulator to generate first-order diffracted beam. The modulator was driven by combination of a pulse generator (Model 8011A, Hewlett-Packard) and a delay generator (Model DG535, Stranford Research Systems). Thus, pulse trains of variable length, pulse separation, and pulse number could be obtained. By selecting the separation time, we refer to this as the time coding, we produced an image of the particle trajectory as series of dots and dashes. From this coded image, the velocities of particles near the cavitation bubbles could be determined. The modulated laser beam was focused horizontally by a bi-convex lens with a focal length of 38.1 mm and expanded vertically by a cylindrical lens with 40 mm focal length. A light sheet of 10 mm height and $200\,\mu$m thickness was produced that passed through the center of the cavitation bubble. The particle track images were captured with a CCD camera (XC-57, Sony) through a microscope (SZ6045, Olympus). The camera was oriented perpendicular to the light sheet. The direction of particle trains was determined by setting different intervals between the last pulse and previous sequential pulses (see Figure 3).

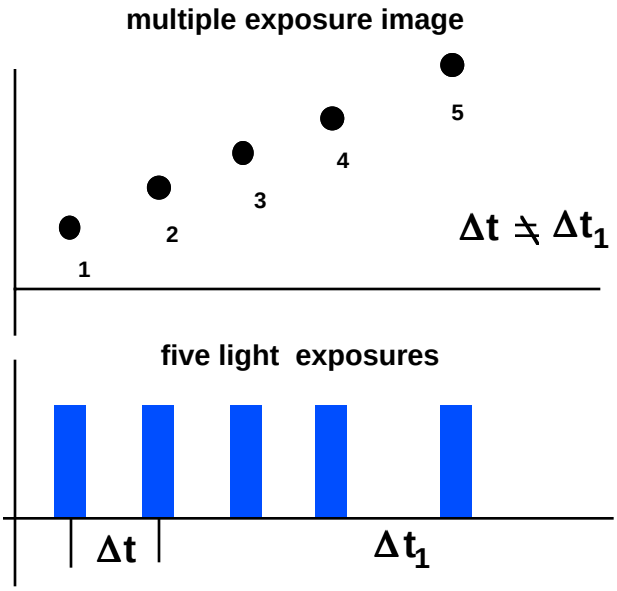

Figure 3: Technique for determining the direction of displacement between exposures on a single frame.

2.6 Flash Photography

Conventional single event flash photography was used to orient each PIV image. Each picture was a single event and reproducible. A strobe (MVS–2601, EG&G) was used for illumination at an adjustable delay time controlled by the digital delay generator. The generator was triggered by the laser pulse using a photodiode (UDT Instruments) that was attached to the laser delivery fiber. The delay time was defined as the period between the end of the laser pulse and the peak of the flash of light from the strobe. The fluid was not seeded for flash photography.

3 Results

We investigated the cavitation bubble dynamics during the bubble expansion, collapse, and several milliseconds after the collapse using PIV. The experiments were separated into those with laser absorption on the gelatin target and those with absorption at the fiber tip.

Figures 4–6 show the PIV/flash photography for the laser absorption on gelatin. Figure 4 shows a multiple exposure photograph of the flow around a cavitation bubble and corresponding flash photography. The flow around the bubble was moving away from the gelatin surface along with the bubble expansion. The measurements indicated that the velocity of particles near the bubble slowed down significantly when the bubble reached its maximum. The dynamic range was about 5–12 m/s. Figure 5 shows the evolution of the flow near a cavitation bubble during the bubble collapse phase. The maximum velocity during this phase was comparable to that during the bubble expansion. The flow moved away from the gelatin target. Figure 6 shows the flow patterns after a comparatively longer time (several milliseconds) after a laser pulse. The particles moved slowly at an average speed of 0.1 m/s. The presence of several vortices around the fiber tip were observed.

Figures 7–9 show the PIV/flash photography for the laser absorption at the fiber tip. Figure 7 shows a multiple exposure photograph of the flow around a cavitation bubble and corresponding flash photography. Unlike the previous case (laser absorption on target), the flow around the bubble was moving towards the gelatin surface along with the bubble expansion. The measurements indicated that the velocity of particles near the bubble slowed down when the bubble reached its maximum. The dynamic range was about 9–12 m/s. The flow also slowed down to 7 m/s near the boundary (dashed line). Figure 8 shows the evolution of the flow near a cavitation bubble during the bubble collapse phase. The measurements indicated that the velocity of particles near the bubble slowed down to 5 m/s near the boundary (dashed line). The maximum velocity during this phase was comparable to that during the bubble expansion. The flow moved towards the gelatin target. Figure 9 shows the flow patterns after a comparatively longer time (several milliseconds) after a laser pulse. The particles moved slowly at an average speed of 0.2 m/s. The particles moved away from the gelatin surface rather than towards the gelatin surface. The presence of several vortices around the fiber tip was observed.

4 Discussion

This study demonstrated that PIV photography is a useful method for the investigation of the photoacoustic drug delivery process. One can obtain more information about the flow behavior near the cavitation bubble and the target by PIV photography than by the conventional flash photography, especially when the bubble reaches its maximum size and interacts with target. For example, it is impossible to measure what is the velocity of flow as it interacts with target from a conventional flash photograph (c.f., Figure 8). However, it is easy to determine the velocity with PIV photography .

The measurements showed that the particle velocities slowed down as the cavitation bubble reached its maximum size. The velocities of particles also slowed when the flow interacted with a target because of the resistance from the target. The difference in the velocities may provide the crucial information related to photoacoustic drug delivery. The question of how fast the particles must move towards the target to penetrate remains and requires further investigation.

The problem of directional ambiguity was resolved by using multiple exposures with variable pulse separation. This technique permits the unambiguous, instantaneous, two-dimensional measurement of velocity near the laser-induced cavitation bubbles in a single frame.

PIV photography showed clearly that the major direction of hydrodynamic flow changed during the bubble expansion and collapse (i.e., towards the target), and at a certain time after the collapse (i.e., away from the target) as the bubble formed at fiber tip. However, it was not clear whether the majority of flow moved towards the target when the bubble was formed on the target although the flow surrounding the bubble moved along with the bubble during its contraction.

The flow patterns suggested that the drug could be delivered into clot or vessel wall radially no matter where the cavitation bubbles were formed since both laser absorption on the target and at the fiber tip could cause the flow to move radially. The drug could be delivered axially as the cavitation bubble formed at fiber tip (i.e., in a light absorbing liquid). However, whether the drug could be delivered axially when the bubbles were formed on target needs further investigation. This study showed that the laser energy used was significantly different for both laser absorption on the target and at the fiber tip although the maximum velocity was comparable each other. This finding suggests that less energy is needed to generate similar velocity if the bubble is formed at fiber tip, which may benefit some medical applications where the less energy is required.

In conclusion, we demonstrated that PIV photography allows the visualization of photoacoustic drug delivery process. The flow pattern depends on where the cavitation bubbles are formed. The particle velocity near the cavitation bubble range from 0.1–12 m/s. The maximum velocity of particles is comparable to the bubble

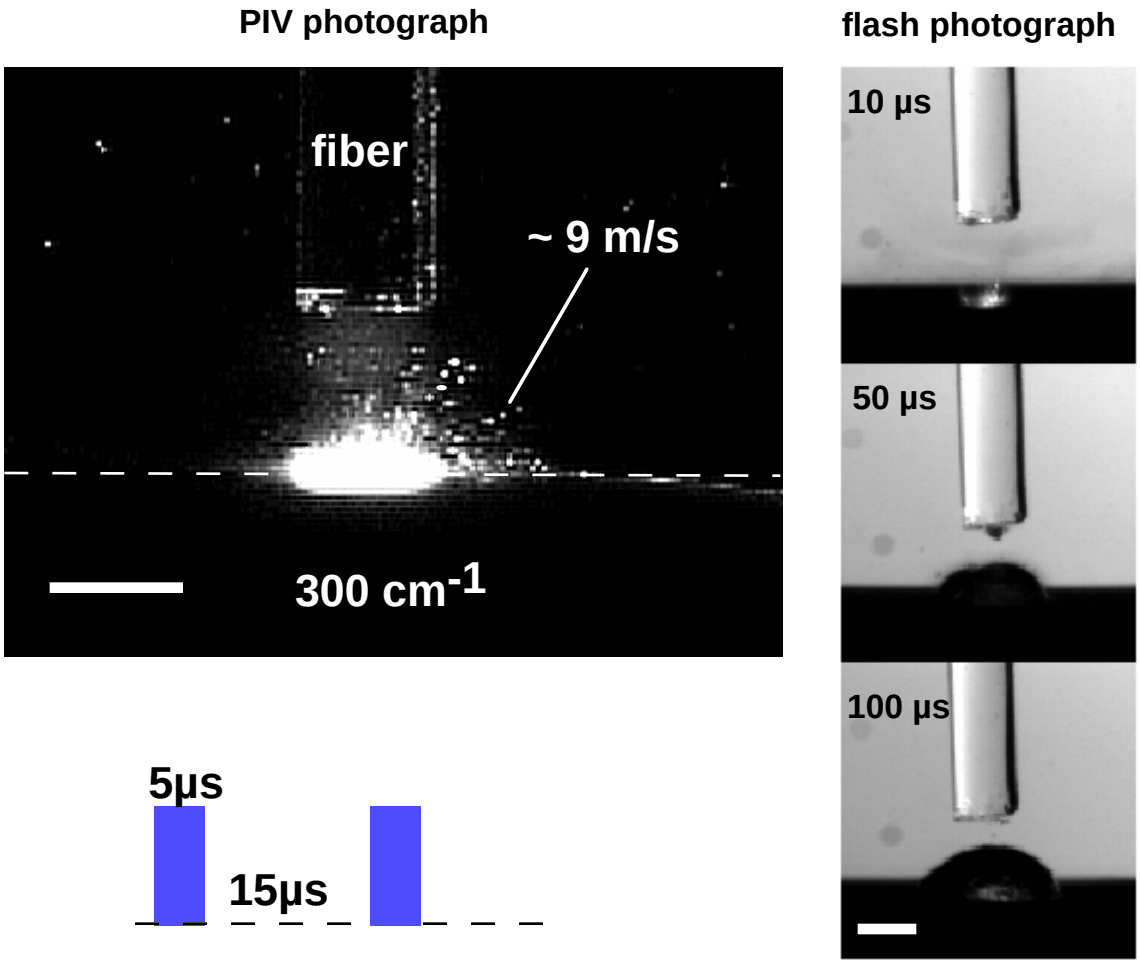

Figure 4: PIV/flash photograph of a cavitation bubble near gelatin target 10–100 μs after a laser pulse. A 60 mJ laser pulse was delivered via a optical fiber with 1000 μm core diameter. The maximum bubble diameter was 2.5 mm at 100 μs. The marked velocity was the average for this specific particle train during the bubble expansion. The white bar presents 1 mm in length. The white dash line indicates the surface of the gelatin target. Five exposures were used with the presented pulse profile.

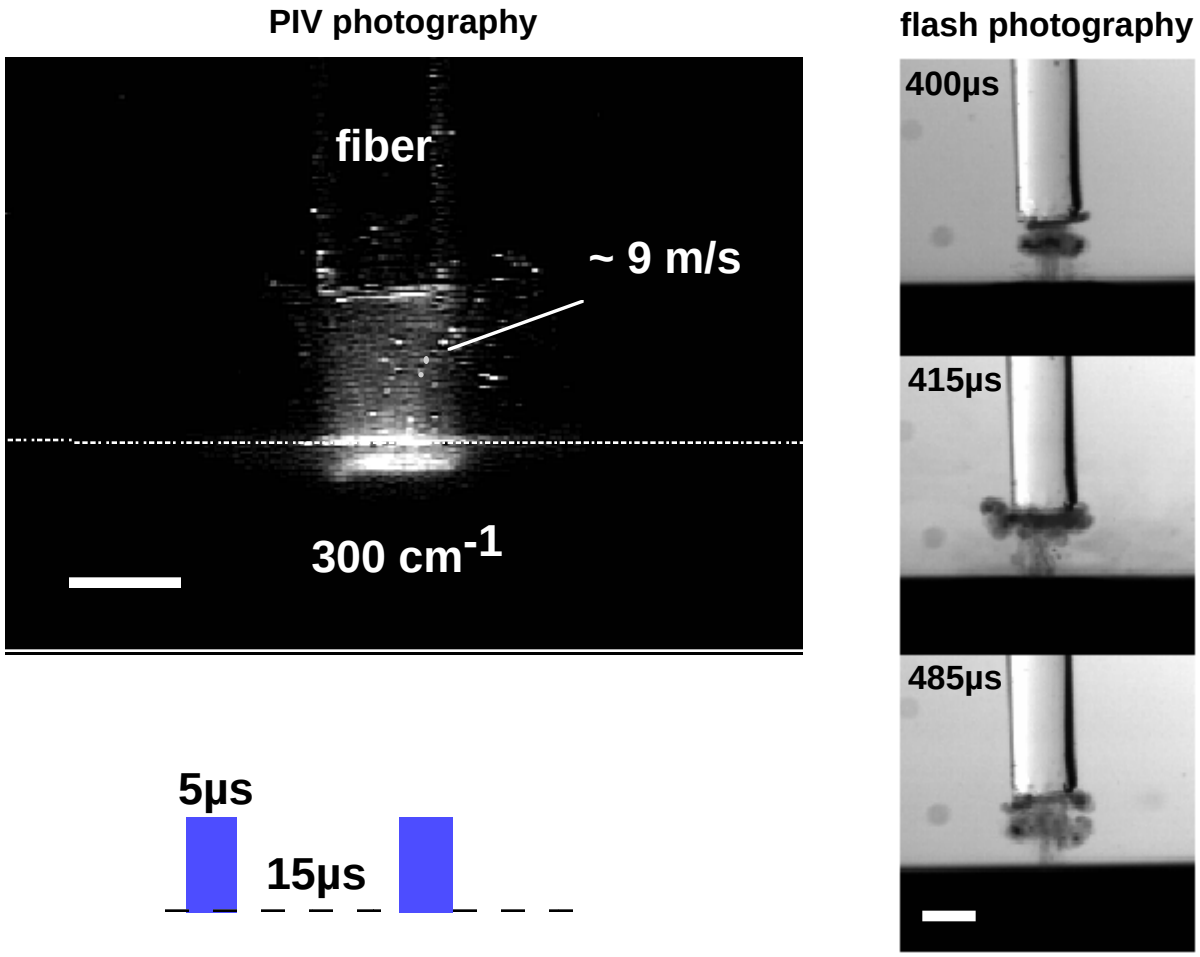

Figure 5: PIV/flash photograph of a cavitation bubble near gelatin target 400–485 μs after a laser pulse. A 60 mJ laser pulse was delivered via a optical fiber with 1000 μm core diameter. The marked velocity was the average for this specific particle train during the bubble collapse. The white bar presents 1 mm in length. The white dash line indicates the surface of the gelatin target. Five exposures were used with the presented pulse profile.

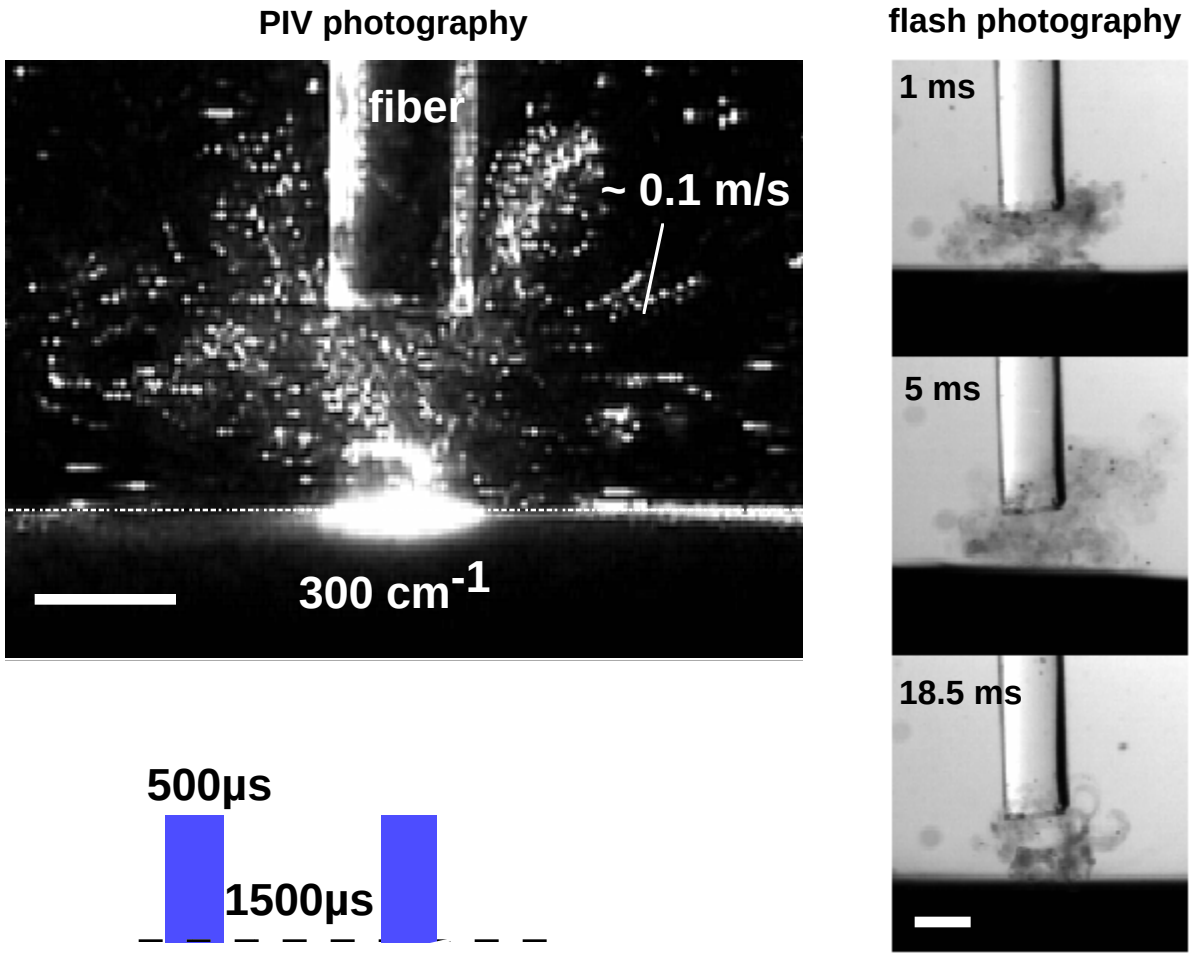

Figure 6: PIV/flash photograph of a cavitation bubble near gelatin target 1–18.5 ms after a laser pulse. A 60 mJ laser pulse was delivered via a optical fiber with 1000 μm core diameter. The marked velocity was the average for this specific particle train during post bubble collapse. The white bar presents 1 mm in length. The white dash line indicates the surface of the gelatin target. Ten exposures were used with the presented pulse profile.

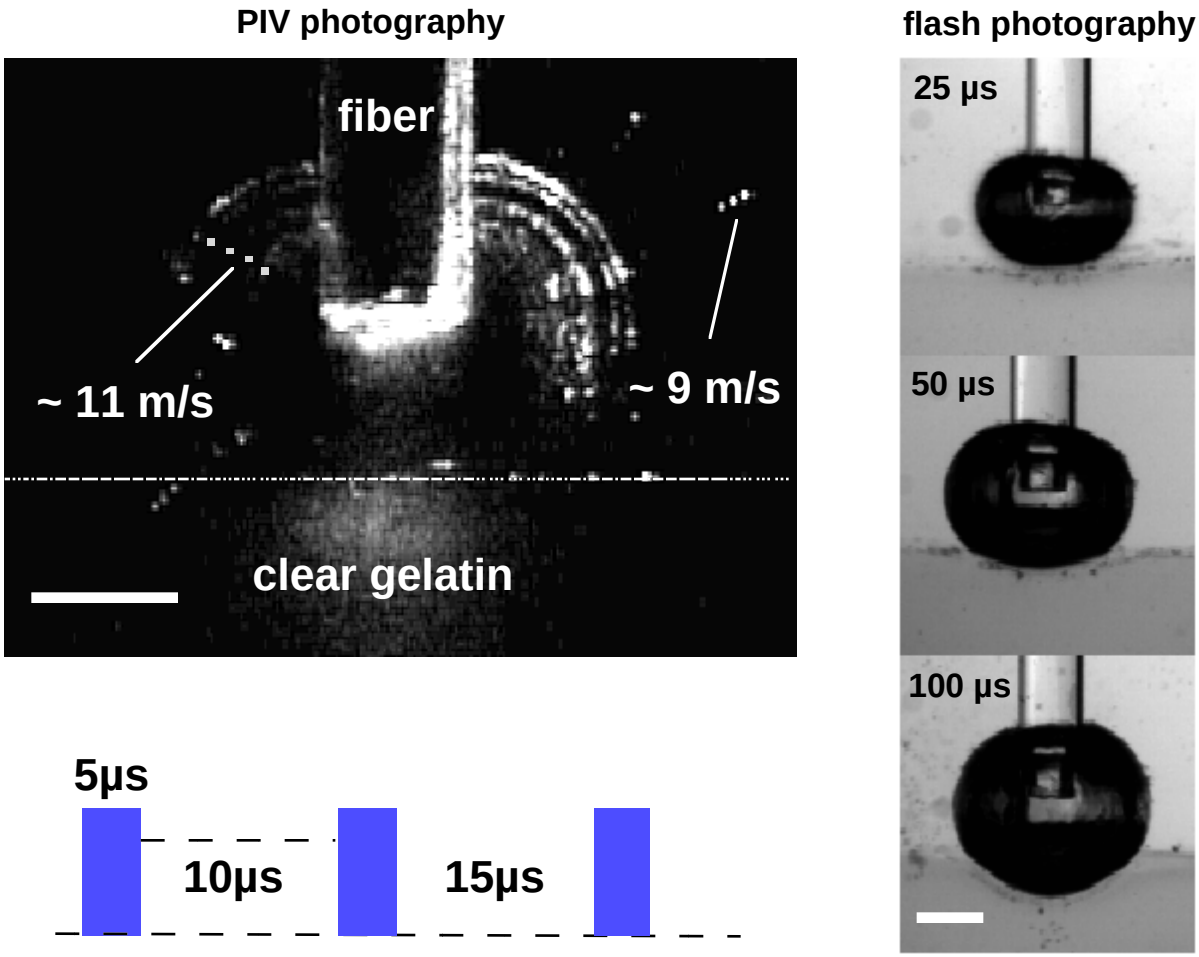

Figure 7: PIV/flash photograph of a cavitation bubble near gelatin target 25–100 μs after a laser pulse. A 30 mJ laser pulse was delivered via a optical fiber with 1000 μm core diameter. The maximum bubble diameter was 3.2 mm at 100 μs. The marked velocity was the average for this specific particle train during the bubble expansion. The white bar presents 1 mm in length. The white dash line indicates the surface of the gelatin target. Five exposures were used with the presented pulse profile.

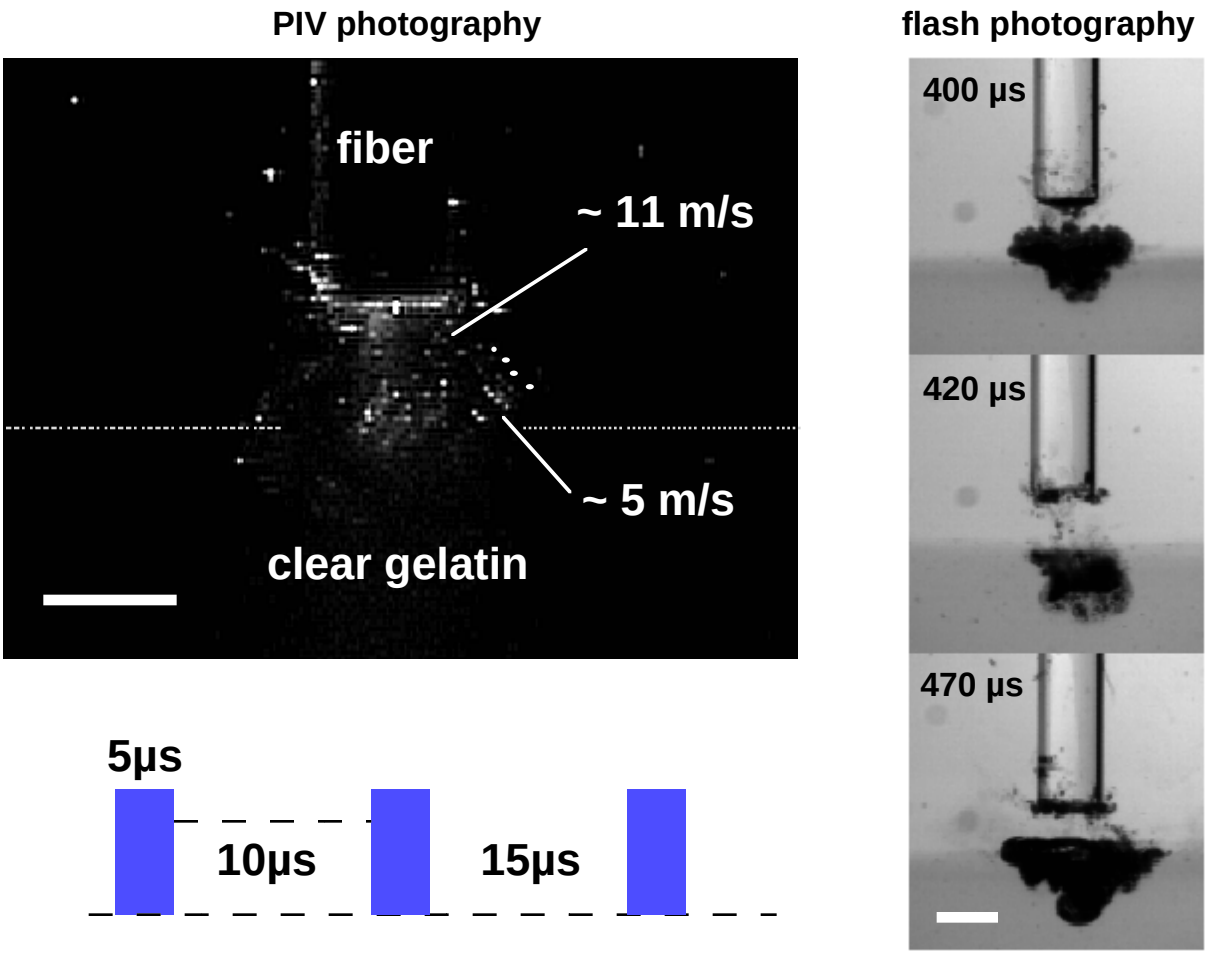

Figure 8: PIV/flash photograph of a cavitation bubble near gelatin target 400–470 μs after a laser pulse. A 30 mJ laser pulse was delivered via a optical fiber with 1000 μm core diameter. The marked velocity was the average for this specific particle trains during the bubble collapse. The white bar presents 1 mm in length. The white dash line indicates the surface of the gelatin target. Five exposures were used with the presented pulse profile.

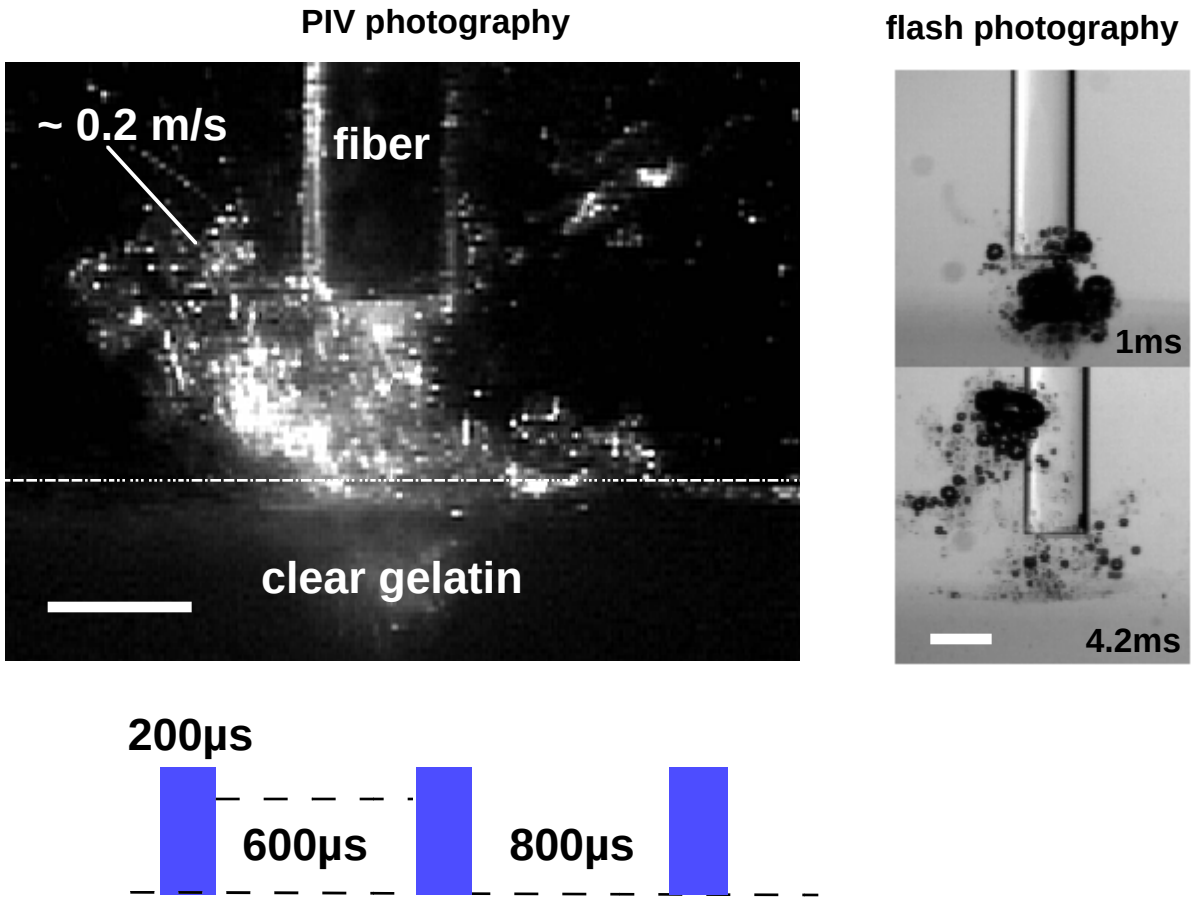

Figure 9: PIV/flash photograph of a cavitation bubble near gelatin target 1–4.2 ms after a laser pulse. A 30 mJ laser pulse was delivered via a optical fiber with 1000 μm core diameter. The marked velocity was the average for this specific particle train during post bubble collapse. The white bar presents 1 mm in length. The white dash line indicates the surface of the gelatin target. Five exposures were used with the presented pulse profile.

expansion and collapse speed.

This work was supported in part by the Murdock Foundation, Portland, Oregon, and the Whitaker Foundation, Washington, DC.

6 REFERENCES

[1] H. Shangguan, L. W. Casperson, A. Shearin, K. W. Gregory, and S. A. Prahl, "Photoacoustic drug delivery: the effect of laser parameters on spatial distribution of delivered drug," in *Proceedings of Laser-Tissue Interaction VI* (S. L. Jacques, ed.), vol. 2391, (San Jose, CA), pp. 394–402, 1995.

[2] H. Shangguan, L. W. Casperson, A. Shearin, and S. A. Prahl, "Visualization of photoacoustic drug delivery dynamics," *Lasers Surg. Med.*, vol. 57, pp. 4–5, 1995 (abstract).

[3] H. Shangguan, L. W. Casperson, A. Shearin, K. W. Gregory, and S. A. Prahl, "Drug delivery with microsecond laser pulses into gelatin," submitted to Applied Optics

[4] W. Lauterborn and H. Bolle, "Experimental investigations of cavitation-bubble collapse in the neighborhood of a solid boundary," *J. Fluid Mech.*, vol. 72, pp. 391–399, 1975.

[5] W. Lauterborn and W. Hentschel, "Cavitation bubble dynamics studied by high speed photography and holography: part one," *Ultrasonics*, vol. 23, pp. 260–268, 1985.

[6] T. G. van Leeuwen, M. J. van der Veen, R. M. Verdaasdonk, and C. Borst, "Noncontact tissuue ablation by holmium: YSGG laser pulses in blood," *Lasers Surg. Med.*, vol. 11, pp. 26–27, 1991.

[7] A. Vogel, R. Engelhardt, and U. Behnle, "Minimization of cavitation effects in pulsed laser ablation - illustrated on laser angioplasty," *Appl. Phys. B*, in press

[8] K. Rink, G. Delacrétaz, and R. P. Salathé, "Fragmentation process of current laser lithotriptors," *Lasers Surg. Med.*, vol. 16, pp. 134–146, 1995.

[9] A. A. Oraevsky, R. Esenaliev, S. L. Jacques, and F. K. Tittel, "Laser flash photography of cold cavitation-driven ablation in tissues," in *SPIE Proceedings of Laser-Tissue Interaction VI* (S. L. Jacques, ed.), vol. 2391, pp. 300–307, 1995.

[10] A. Vogel and W. Lauterborn, "Time-resolved particle image velocimetry used in the investigation of cavitation bubble dyanmics," *Appl. Opt.*, vol. 9, pp. 1869–1876, 1988.